AECL EACL

CA9900196

AECL-11842

Transient Fission-Product Release During Reactor Shutdown and Startup

Libération de produits de fission transitoires au cours de l'arrêt et du démarrage du réacteur

C.E.L. Hunt, B.J. Lewis, L.W. Dickson

December 1997 décembre

AECL

TRANSIENT FISSION-PRODUCT RELEASE DURING REACTOR SHUTDOWN AND STARTUP

by

C.E.L. HUNT[1], B.J. LEWIS[2] and L.W. DICKSON

[1]Former AECL employee. Present address, P.O. Box 958, Deep River, Ontario, K0J 1P0.
[2] Royal Military College of Canada, Department of Chemistry and Chemical Engineering, Kingston, Ontario, K7K 5L0.

Fuel Safety Branch
Chalk River Laboratories
Chalk River, Ontario K0J 1J0

1997 December

AECL-11842

EACL

LIBÉRATION DE PRODUITS DE FISSION TRANSITOIRES AU COURS DE L'ARRÊT ET DU DÉMARRAGE DU RÉACTEUR

par

C.E.L. HUNT[1], B.J. LEWIS[2] et L.W. DICKSON

[1] Ancien employé d'EACL. Adresse actuelle : C.P. 958, Deep River (Ontario) K0J 1P0
[2] Collège militaire royal du Canada, département de Chimie et de Génie chimique, Kingston (Ontario) K7K 5L0

RÉSUMÉ

L'analyse des résultats des expériences par gaz de balayage, réalisées aux Laboratoires de Chalk River d'EACL de 1979 à 1985, a été poursuivie afin de déterminer la fraction de produits de fission gazeux qui est libérée lors de l'arrêt et du démarrage du réacteur. Des équations empiriques ont été déduites et appliquées pour calculer la libération de xénon stable des éléments combustibles associés et d'une grappe de combustible expérimentale bien documentée irradiés dans le réacteur NRU. On a pu faire correspondre la libération de gaz calculée aux valeurs mesurées à un facteur de près de deux dans le cas d'une expérience d'irradiation avec une combustion massique de 217 MWh/kgU.

Il y avait aussi des renseignements restreints sur la fraction de l'iode radioactif qui était exposé, mais non libéré, lors de l'arrêt du réacteur. On propose une équation empirique pour calculer cette fraction.

Sûreté du combustible
Laboratoires de Chalk River
Chalk River (Ontario) K0J 1J0

1997 Décembre

AECL-11842

AECL

TRANSIENT FISSION-PRODUCT RELEASE DURING REACTOR SHUTDOWN AND STARTUP

by

C.E.L. HUNT[1], B.J. LEWIS[2] and L.W. DICKSON

[1]Former AECL employee. Present address, P.O. Box 958, Deep River, Ontario, K0J 1P0.
[2] Royal Military College of Canada, Department of Chemistry and Chemical Engineering, Kingston, Ontario, K7K 5L0.

ABSTRACT

Sweep-gas experiments performed at AECL's Chalk River Laboratories from 1979 to 1985 have been further analysed to determine the fraction of the gaseous fission-product inventory that is released on reactor shutdown and startup. Empirical equations were derived and applied to calculate the stable xenon release from companion fuel elements and from a well-documented experimental fuel bundle irradiated in the NRU reactor. The calculated gas release could be matched to the measured values within about a factor of two for an experimental irradiation with a burnup of 217 MWh/kgU.

There was also limited information on the fraction of the radioactive iodine that was exposed, but not released, on reactor shutdown. An empirical equation is proposed for calculating this fraction.

Fuel Safety Branch
Chalk River Laboratories
Chalk River, Ontario K0J 1J0

1997 December

AECL-11842

TABLE OF CONTENTS

1. INTRODUCTION

From 1979 to 1985, a total of six sweep-gas experiments were done in the NRX reactor at the Chalk River Laboratories of Atomic Energy of Canada Limited. The first two experiments were designed to measure the steady-state release rate of fission gases from UO_2 fuel [1-3]. Later experiments were designed to measure the effects of severe transients such as loop blowdown [4-8]. During the course of the irradiations there were many reactor shutdown and startup transients, and for some of these the fission-product release was monitored continuously by on-line γ-ray spectrometers.

Re-examination of the records showed that two experiments, designated FIO-133 and FIO-134, had good shutdown and startup data. Two others, FIO-122 and FIO-124, had some useable data, primarily for startups. Table 1 lists the basic parameters for these four experiments.

During the first two experiments, FIO-122 and FIO-124, counting times for the γ-ray spectrometer were generally long, in order to obtain good counting statistics for steady-state release rates. As a result, details of the transient releases during shutdown and startup were generally lost. When counting times were deliberately reduced to obtain shutdown data, it was found that the high radiation fields saturated the spectrometer. Thus, the magnitudes of the peak releases were lost. The later experiments, FIO-133 and FIO-134, used smaller collimators and the saturation problem was almost eliminated. Also, for a few shutdown and startup transients, the counting times were reduced to as little as 45 s, giving excellent dynamic measurements. For the current analysis, it was found that the latter two experiments gave the most reliable data. Because of the spectrometer saturation difficulties, particularly on shutdown, data were consistently lost during the first two experiments.

2. EXPERIMENTAL

The sweep-gas circuit and the data-reduction techniques have been thoroughly described elsewhere [3]. Details of the four fuel assemblies are listed in Table 1 and are briefly described below.

In the FIO-122 experiment, the fuel element operated at a nominal linear power of 43 kW/m to a burnup of 86 MWh/kgU. Irradiation was halted because the swept element developed a defect. Counting times tended to be long, so little detail was obtained on the transient shutdown release. Of the total of 27 startup and shutdown cycles, fission-product release was measured during six transients and on three occasions an attempt was made to measure the dynamics of the shutdown release. Counting times were shortened, but spectrometer saturation occurred. This resulted in loss of data from the shutdown peak. Since the reactor startup rate was much slower than the shutdown rate, the peak release was also lower and there was less spectrometer saturation. As a result, startup releases were generally more reliable. Again, long counting times resulted in loss of detail of the release kinetics. Details of fuel power and burnup at each shutdown were estimated from plots of the reactor power.

The fuel element in the FIO-124 experiment operated at a nominal linear power of 60 kW/m to a burnup of 50 MWh/kgU. Again, irradiation was halted because the swept element defected. There were 18 reactor startups and shutdowns during the experiment. Data were recorded during 11 shutdowns and 11 startups. Similar problems of spectrometer saturation during the shutdowns were experienced as for FIO-122. The fuel power and burnup at each transient were estimated from plots of the reactor power.

FIO-133 was the first of the experiments planned for transient tests. There were 30 startup and shutdown cycles, three of which were high-temperature transients. The fuel element operated at a power varying from about 52 to 62 kW/m to a burnup of 55 MWh/kgU.

Collimator modifications minimized the problem of spectrometer saturation and counting times were generally reduced, in some cases to as short as 45 s. As a result, the shutdown data were generally good. However, some of the shutdowns were short, less than 1 h, and there is evidence from the long-lived isotopes that all of the fission gases had not been fully vented by the time the reactor started up again. As a result, the measured release on shutdown is probably low for these short transients. Fuel power and burnup at each shutdown were obtained from the on-line data-acquisition system.

FIO-134 was a high-burnup experiment in which the fuel element operated at a linear power varying from 51 to 61 kW/m, with the average close to 54 kW/m, to a burnup of 200 MWh/kgU. At this burnup, the sweep gas was changed from inert to oxidizing and irradiation continued to a burnup of 227 MWh/kgU. Data were obtained for 12 shutdowns and 10 startups. The fuel power and burnup were taken from the on-line data-acquisition system.

3. ANALYSIS

Figure 1 shows one of the shutdown-startup transients for FIO-133 where counting times were 45 s. The isotopes ^{133}Xe and ^{85m}Kr have been selected as examples to show the general behaviour. There is evidence of spectrometer saturation during at least the first two data points shown after the reactor shutdown, where the release rate first increases and then decreases before reaching the peak value. The reactor startup occurred in steps, and this is reflected in the startup release rates. There is no evidence that the release rates during startup were high enough to saturate the spectrometer.

The release-rate data for each shutdown and startup were analysed using spreadsheets. Releases for each isotope were integrated over the particular transient. The isotopic inventories were calculated from the steady-state operating power immediately prior to the shutdown. The rate of change of the number of atoms of a given isotope present in the UO_2 fuel element may be expressed by:

$$dN/dt = B - R - \lambda N \qquad (1)$$

$= 0$ at steady state

where: N = number of atoms in the fuel,
B = number of atoms born per second,
R = number of atoms released per second,
λ = decay constant of the isotope (s^{-1}).

Therefore, at steady-state conditions:

$$N = (B - R)/\lambda \quad (2)$$

Let the number of atoms released during the transient be n,

where $$n = \int_{transient} R(t)\, dt \quad (3)$$

A transient release fraction can then be defined by

$$n/N = \lambda \int_{transient} R(t)\, dt \,/\, (B - R) \quad (4)$$

Both N and n are dependent on the fission-product inventory, and as a result their ratio should be independent of λ. This was found to be generally true, although there was considerable scatter. Part of the scatter may be because the peak searching program was not always consistent. Sometimes the peak used to detect a given isotope would be missed on a particular spectrum. When counting times were long, this could have a major impact on the calculated integral. The original spectra were not available to redo the peak search. For some isotopes, where multiple strong peaks were available for analysis, the missing data could be estimated.

As may be seen from Table 1, the fuel elements for the four experiments had different dimensions. The larger-diameter pellets of FIO-133 seem to have had little effect on the results, which have been expressed as release fractions. We were able to consider all experiments as one data set. The fuel stack lengths were also different, 378 mm for FIO-133 and 477 mm for the others. This requires particular care to make sure that all the calculations are dimensionally correct. The birth rate was calculated as a constant (depending on the isotope) times fuel power. However, fuel power is typically quoted as kilowatts per meter of fuel length, and this is the preferable way for comparing results from different experiments. Releases, on the other hand, were measured as total atoms per second from the fuel element. For convenience, all release rates were converted to atoms/s per meter of fuel length.

Figure 2 shows one example of the calculated release fraction for each isotope plotted against the decay constant. The isotopes where there is a large contribution from the iodine precursors, ^{133}Xe, ^{135m}Xe, and ^{135}Xe consistently showed a higher release rate than those without long-lived precursors. The contribution of the precursor can be estimated by extrapolating the long-term release rate of the xenon, after the gas has been released and the rate is controlled by the decay of the iodine, back to the time of the shutdown. The integral below this line should be the

contribution to the signal from the precursor. In the example of Figure 2, this correction brought the results for ^{133}Xe and ^{135}Xe in line with the other isotopes. It was insufficient to reduce the ^{135m}Xe release fraction to match the remaining data. In general, even after correction for the iodine precursor, the ^{133}Xe and ^{135m}Xe calculations were still high, while ^{135}Xe was low.

Release fractions for isotopes with half-lives shorter than ^{137}Xe (3.83 min) were also often apparently in error. The transport time from the fuel to the spectrometer was usually at least 200 s. This is five or more half-lives for ^{139}Xe and ^{90}Kr. A small error in calculating the transport time will have an increasing effect on the calculated release rate as the half-life of the isotope decreases. This is evident in Figure 2, where the isotopes ^{137}Xe and beyond show a consistent trend of increasing over correction as the half-life decreases.

The shutdown release fraction was found to depend strongly on both fuel power and burnup. With the exception of very low burnup, less than about 5 to 10 MWh/kgU, where the fuel is still sintering, both dependencies are seen to increase exponentially.

3.1 Power Dependence of Shutdown Release

The analysis was complicated because of the strong dependence of the release on both power and burnup. Initially, data were examined from all four experiments, divided into small ranges of burnup. Unfortunately, so much data was lost because of spectrometer saturation in FIO-122 and FIO-124 that comparisons of release fraction versus power using data for all four experiments proved impossible. Finally, six shutdowns from FIO-133 spanning a burnup range from 41 to 48 MWh/kgU and a power range from 47 to 62 kW/m were selected. Spectrometer saturation still occurred, but appeared to be restricted to one, or at most two, counting cycles, certainly less than 2 min total. It was assumed that the proportion of the data lost in this manner was small compared with the overall integral.

The next problem was to select representative isotopes where there was a strong gamma-ray signal and little chance of interference from extraneous peaks. The data for the ^{85m}Kr γ-ray peak at 151.2 keV with an abundance of 0.755 were finally selected as probably being the most reliable. The ^{88}Kr gamma ray at 196.3 keV with a gamma abundance of 0.26 was chosen as a check. ^{133}Xe was rejected because the data were badly scattered and the 81 keV gamma ray is subject to interference from ^{131}I. There is also a problem from the contribution of the precursor ^{133}I. ^{135}Xe was also rejected because of complications caused by the long-lived iodine precursor and neutron-absorption effects.

The results are shown in Figure 3. The slope of the regression line calculated through the ^{85m}Kr data was 7 and that through the ^{88}Kr data was 6. The data points above 60 kW/m are for the burnup ranging from 41 to 42 MWh/kgU. The one at 50 kW/m was at 48 MWh/kgU, and the one at 47 kW/m is for a burnup of 45 MWh/kgU. An average value between the ^{85m}Kr and ^{88}Kr power dependence of 6.5 is probably reasonable. This value was used for the next stage of the analysis. Considering the scatter of the data shown in Figure 3, the error on this exponent is probably of the order of $\pm$1.5; i.e., a maximum value of 8 and a minimum value of 5.

3.2 Burnup Dependence of Shutdown Release

Having established a power dependence using a limited data set, where the burnup was almost constant, we used all of the data from experiments FIO-133 and FIO-134 to establish the burnup dependence. The power was standardized to 55 kW/m using the power dependence of 6.5. Again, most weight was given to the isotopes ^{85m}Kr and ^{88}Kr. Figure 4 shows the results. After the initial sintering portion of the curve, shown by the rapidly decreasing release of the first three points up to about a burnup of 10 MWh/kgU, an upper bound burnup dependence of 2.4 appears to fit the data for ^{85m}Kr (Figure 4(a)). Some data fall below the line, because of incomplete release due to the short time between a shutdown and the following startup. The same slope is a good representation for ^{88}Kr (Figure 4(b)). This slope was then applied to the other isotopes and, as can be seen in Figure 5, it provides a reasonable prediction for ^{133}Xe and ^{135}Xe. However, much of the xenon data for FIO-134 appears to be low. Again, this is probably because the shutdowns were of short duration and not all of the available fission gases had been released when the reactor started up. Overprediction was more apparent in FIO-134 than in FIO-133, possibly a consequence of the difference in pellet size between the two experiments. Inspection of the data in Figures 4 and 5 suggests that the error on the exponent of 2.4 should not be much more than about ±0.5.

Figures 6(a) and 6(b) show the same data as Figures 4(a) and 5(a), but with a linear burnup scale. The sintering phase with a decrease in the release of 2 to 3 decades followed by a continuously increasing release fraction with burnup is more apparent, as is the scatter in the FIO-134 data at high burnup. The correlation curve is generally conservative, providing an upper-bound for the release fraction.

From the above analysis, we now have a dependence of the release fraction, F, (n/N in Eq. (4)) on both fuel operating power and burnup. We may write the correlation as follows:

$$F_{SD} = 2.2\ (10^{-19})\ P^{6.5}\ B^{2.4} \qquad (B \geq 10\ \text{MWh/kgU}) \qquad (5)$$

where the power, P, is in kW/m and the burnup, B, is in MWh/kgU.

Figure 7 shows the release fraction for five isotopes based on the results shown in Figures 4 and 5, calculated for 55 kW/m fuel power and a burnup of 100 MWh/kgU. A line independent of the decay constant is not unreasonable. The constant in Eq. (5) was evaluated by substituting the value from Figure 7 into the above equation for a power of 55 kW/m and a burnup of 100 MWh/kgU.

We thus have an empirical equation for the release fraction of fission products resulting from a shutdown. Since the release fraction is constant for all isotopes, we also have a measure of the release fraction of stable isotopes. These are the ones which will result in buildup of gas pressure in the fuel-to-sheath gap. With Eq. (5) we should be able to calculate the pressure buildup due to

shutdowns for any fuel element for which the power, burnup and shutdown history is known. However, as shown in Figure 1, there is also a comparable release on reactor startup.

3.3 Startup Release Analysis

Having established the release behaviour resulting from the shutdown, it is now necessary to determine the release that occurs on startup. Noting that the fuel cracked on shutdown, releasing stored inventory, there are two possible explanations for the release on startup. Firstly, at least a part of the startup release peak that is observed will be by diffusion from the increased surface area, until sintering heals the cracks. Secondly, additional cracking occurs, because of thermal stresses generated by the return to power, in which case additional stored inventory will be released as well.

The peak release for all but the very shortest-lived isotopes, which required time to build up a measureable inventory, occurred well before the reactor had reached full power. The actual fuel power at the time the maximum release rate was measured was obtained from operating history records for both FIO-133 and FIO-134. The measured peak release rate was compared with the steady-state release rate for the same conditions (i.e., power and burnup). This required an analysis of the steady-state behaviour.

3.3.1 Steady-State Release Rates

Again, we are faced with the problem of analyzing something which depends simultaneously on two variables, power and burnup. We also have experiments where there were different swept areas (number and size of grooves) and fuel length. Again, ^{85m}Kr was chosen as the isotope to place the most reliance on, being the one with the strongest gamma-ray signal that is clear of interference from other gamma rays, and one with a reasonable half-life.

The steady-state release rates for all four experiments and all isotopes were plotted as a function of burnup. Figures 8(a) and 8(b) show the results for ^{85m}Kr and ^{133}Xe, respectively. The release rates have been normalized to identical fuel lengths, 477 mm, and identical swept areas of six grooves, 1.15 mm x 1.15 mm.

Best-estimate lines were drawn through the data for each isotope, and the slope calculated. The estimated slopes varied from a low of 0.71 for ^{135}Xe to a high of 0.94 for both ^{87}Kr and ^{88}Kr. The value for ^{85m}Kr (i.e., the isotope that is considered to be the most reliable) was approximately 0.8. However, this only applies to a burnup greater than about 10 MWh/kgU. At very low burnup, the effects of sintering of the fuel, discussed earlier in reference to the shutdown releases, also apply.

Having established a burnup dependence for the steady-state release rate, the next step was to calculate a power dependence. Using a burnup dependence of 0.8, the steady-state release rates were normalized to a nominal burnup of 50 MWh/kgU and plotted as a function of fuel power. The results for ^{85m}Kr and ^{133}Xe are shown in Figures 9(a) and 9(b). Best-estimate lines were

again drawn through the results for each isotope. The slopes varied from about 3.7 to 5. Since ^{85m}Kr is expected to give the most reliable data, the lower value is probably closer to the correct value.

3.3.2 Startup Release Fraction

The lines shown in Figures 9(a) and 9(b) were used to estimate the steady-state release rate that would be expected for each isotope at the fuel power when the peak startup release rate was observed.

Figure 10 shows the ratio of the observed startup peak release rate to the steady-state release rate (i.e., the rate that is predicted to occur at the power at which the peak release rate was observed) versus the fraction of inventory of the isotope remaining when the reactor started up. This has been done for six short-lived isotopes.

The long-lived isotopes like ^{133}Xe generally show peak release rates hundreds or thousands of times greater than the expected steady-state value for the same fuel power. However, for almost all startups, the fraction of inventory remaining at startup was large for these isotopes; i.e., usually greater than 0.95. Figure 10 shows the ratio for isotopes where the remaining inventory on startup was usually very much less. The scatter is large, as would be expected, considering all the uncertainties in picking steady-state release rate values from Figure 9, and in calculating the remaining inventory of short-lived isotopes when the shutdown period is probably little better known than to the nearest 5 to 10 min. With these reservations both on the ratio and on the calculated fraction of the inventory remaining at startup, Figure 10 shows that as the remaining inventory increases, the ratio of peak to steady-state release increases. Therefore, there must be additional fuel cracking on startup, and hence release of stored inventory. This is consistent with the very high ratios calculated for the long-lived ^{133}Xe.

The data for ^{133}Xe were plotted separately in Figure 11 as the ratio of the peak release rate to the steady-state release rate versus the fuel power at the time the peak release was measured. Figure 11 shows no clear dependence on the fuel power. As a result, we conclude that the amount of fuel cracking that occurs on startup is an inherent characteristic and is not power-dependent, at least for powers greater than 40 kW/m. This is not surprising if one considers that the fuel temperature depends on fuel power, and that above some temperature the UO_2 will become plastic and no longer crack due to imposed thermal stresses. Thus we could expect that the fuel will always crack on reactor startup until the appropriate power, and hence temperature, is reached.

Having established that additional cracking does occur on startup, the next problem is to try to calculate the magnitude of the release, particularly for the stable fission gas.

3.3.3 Stable Fission-Gas Release on Startup

It was assumed that the stable fission-gas release on startup would be most closely approximated by that of ^{133}Xe. Those startups were selected where the most detail, shortest counting times, were obtained, so that there was a reliable value for the integrated release. Six startups were selected from each of FIO-133 and FIO-134. This integrated peak was corrected by dividing by the fraction of the inventory remaining at the time of reactor startup. A release fraction for startup was then calculated by dividing the corrected startup release by the pre-shutdown inventory. The results are shown in Figure 12 superimposed on the shutdown release fraction curve from Figure 6(b).

There are two anomalies. The first data point for FIO-133 is low, but this may be because of the low burnup of 27 MWh/kgU. The datum for FIO-134 at 123 MWh/kgU, which is high by an order of magnitude, cannot be explained. The remaining data scatter about a line that suggests that the startup release fraction is independent of burnup, with a value of about 8×10^{-4}. By inspection of the limited data in Figure 12, an error of plus or minus a factor of two on this value is probably reasonable.

4. MODEL APPLICATIONS

We now have values for the release behaviour both on shutdown and startup. On shutdown, the release fraction is independent of the decay constant, as expected. It is dependent on the fuel operating power and on the burnup, and may be expressed by Eq. (5).

The release fraction on startup is independent of either power or burnup, and may be expressed by the constant value obtained from Figure 12:

$$F_{SU} = 8 \times 10^{-4} \qquad (6)$$

It has been shown from both the sweep-gas tests [5,6] and in-reactor tests, where a pressure transducer continuously measured the internal fuel-element gas pressure, reported by Notley et al. [9], that the gas release during steady-state operation is negligible compared with the release during power transients. The above two expressions, therefore, should give us a way of calculating the stable gas release expected from a fuel element based on its known power history. This was done for FIO-122 and FIO-124, where post-irradiation gas-puncture measurements were done on companion fuel elements. In addition, gas-puncture results were available from several of both outer and inner elements of the experimental fuel bundle designated as bundle SCA, which was irradiated in NRU in 1966 and 1967. It was irradiated to a calculated burnup of 150 MWh/kgU on the inner elements and 220 MWh/kgU on the outer elements. Power and burnup data and the startup/shutdown history were obtained from the reactor operating logs. The gas-puncture data were reported previously [10].

The results are summarized in Table 2. Since we are calculating the fraction of the total amount of stable gas that is released, the most important shutdowns are those that occur towards the end of the irradiation. There were a total of 27 shutdowns during the irradiation of FIO-122, 18 for FIO-124 and 117 for bundle SCA. The results for FIO-122 are within the measured range, for FIO-124 they are slightly low, and for fuel-bundle SCA the calculated release for both the inner and outer elements is too high.

The history for bundle SCA showed that there were many shutdowns, particularly towards the end of the irradiation, where the time at power between a startup and the next shutdown was short (in some cases less than 1 h). There were two shutdowns for FIO-133 at a burnup of about 8 MWh/kgU with only 3 h between reactor startup and the second shutdown. The number of atoms released on the second shutdown was nearly two orders of magnitude lower than would be expected compared with shutdowns occurring after about 100 h or more at power.

Metallographic evidence from FIO-122 showed that cracks created in the UO_2 will resinter during subsequent irradiation. We postulate that if the fuel has only been at power for a short time before there is another reactor shutdown, the cracks produced in the UO_2 during the previous shutdown/startup cycle will not have had time to heal, and the thermal stresses resulting from the new shutdown will tend to make cracks follow the paths of the previous, unhealed cracks. Thus there would be little new inventory released, since it had already been released by the previous shutdown and startup. The question is, how much time at power is required to complete resintering?

Examination of the plots of release rate as a function of time showed that ^{135}Xe was probably the best isotope to analyze to determine the sintering kinetics. The signal is strong and unambiguous. Five startups from FIO-133 and six from FIO-134 were examined, and the times to return to equilibrium were estimated directly from the plots. The times obtained for each experiment and the operating fuel power at each of these startups were averaged. Plots were not available for the other two experiments, so times were estimated from the computer printout of the release rates. Only two startups from FIO-124 were suitable (i.e., the spectrometer was on for a long enough time after startup to unambiguously determine when equilibrium had been reached), and one from FIO-122. The results are shown in Figure 13. In spite of large scatter between individual measurements, the averages, as plotted, show remarkable consistency. These are probably overestimates of the time required to resinter, because the reactor power is usually raised in steps, so that full power is reached some time after the nominal time of the startup.

The next question is, how much do the cracks have to resinter before the next shutdown will result in new cracks following a new path, and again release inventory stored in the grain-boundary bubbles? We know that about 3 h at a nominal power of 52 kW/m is insufficient since, as discussed above, the release was nearly two orders of magnitude lower than expected. Unfortunately, we have no other useful data. The time required for complete resintering is almost certainly an overestimate. From Figure 13, the 3-h data point is about 1/8 of the time required for complete resintering at 52 kW/m. Increasing the fraction of resintering required before cracks follow a new path made the predictions for both FIO-122 and FIO-124 worse, but

improved them for fuel-bundle SCA. Three-quarters of the time required for complete resintering was taken as a reasonable compromise. Thus, it is assumed in the present simulation that no additional stored gas is released on shutdown or startup if the time between the previous startup and the given shutdown is less than three-quarters of that estimated to produce complete resintering (see Figure 13). The results are summarized in Table 2.

5. FRACTION OF IODINE EXPOSED ON SHUTDOWN

There are limited data to determine the amount of iodine exposed on crack surfaces created by the shutdown. The requirement is a long shutdown so that all of the gas is released and the ^{133}Xe, ^{135}Xe and ^{135m}Xe release rates are controlled by the disintegration of their iodine precursors. The release rate, R_{Ni}, for the given noble gas isotope is then extrapolated back to the time of the shutdown,

$$R_{Ni} = f_i \lambda_{Ii} N_{Ii} \qquad (7)$$

where f is the branching fraction for the particular decay scheme. The total number of iodine atoms exposed, N_I, is easily deduced from Eq. (7). The fraction of iodine exposed was calculated by dividing N_{Ii} by the steady-state inventory, obtained from Eq. (2). There were four such shutdowns for FIO-122, one for FIO-124, four for FIO-133 and three for FIO-134. It was assumed that the mechanism exposing fuel surfaces covered with iodine would be the same as that which releases fission gases from the stored inventory in bubbles. Thus, the same power and burnup dependence was assumed. The results are shown in Figures 14(a) and 14(b). The scatter, particularly for the power dependence, is considerably greater than for the gases.

The fraction of the iodine inventory exposed after the shutdown may be expressed by the following relation:

$$F_I = 7(10^{-18})\, P^{6.5}\, B^{2.4} \qquad (8)$$

This gives a fraction exposed of about 32 times the equivalent release of xenon or krypton calculated from Eq. (5). This suggests that the steady-state diffusion coefficient of iodine is higher than that of the noble gases, by a factor of about 6, in order to have stored twice the fraction of iodine on the surfaces exposed by the fuel cracking as the noble gases released from the same cracks. This is in agreement with other estimates [11,12,13].

6. CONCLUSIONS

1. A correlation has been developed to estimate the fraction of the total fission-gas inventory released during reactor shutdown and startup. This work is based on analysis of release rates that were measured for short-lived isotopes in sweep-gas experiments at

Chalk River Laboratories (linear powers from 43 to 60 kW/m, up to a burnup of 200 MWh/kgU).

2. The fission gas released from fuel on reactor shutdown can be estimated based on the operating conditions of fuel power P (in kW/m) and burnup B (in MWh/kgU) prior to the shutdown. The empirical equation derived for the fraction of the steady-state inventory released on shutdown is:

$$F_{SD} = 2.2\ (10^{-19})\ P^{6.5}\ B^{2.4}$$

The shutdown gas-release fraction depends on the extent to which the fuel cracks from the thermal shock. The fuel cracks further on startup and the amount of startup cracking is relatively independent of the fuel power and burnup. A constant value for the fraction of the total inventory released on startup is deduced to be:

$$F_{SU} = 8 \times 10^{-4}$$

3. If the operating time between two consecutive startups is insufficient to resinter the cracks in the fuel, the fractional gas release is orders of magnitude less than that calculated above. About three-quarters of the time estimated to completely resinter may be required before the next shutdown appears to produce cracks which follow a new path through the fuel.

4. The gas release calculated over the lifetime of the fuel agrees within a factor of ≈ 2 with gas-puncture measurements, provided several assumptions are made. The main assumption is that no further gas was released if the time between reactor startup and shutdown was less than three-quarters of that estimated to produce complete resintering of the cracks in the UO_2.

5. The fraction of the iodine inventory exposed due to fuel cracking on reactor shutdown may be expressed by the empirical equation:

$$F_I = 7\ (10^{-18})\ P^{6.5}\ B^{2.4}$$

The steady-state diffusion rate of iodine in UO_2 appears to be about six times that of the noble gases.

7. REFERENCES

1. J.J. Lipsett, I.J. Hastings and C.E.L. Hunt, "Behaviour of Short-Lived Iodines in Operating UO_2 Fuel Elements," CNA 22nd Annual International Conference, 1982 June 6-9. AECL Report, AECL-7721, 1984 November.

2. I.J. Hastings, C.E.L. Hunt, J.J. Lipsett and R.D. MacDonald, "Behaviour of Short-Lived Fission Products Within Operating UO_2 Fuel Elements," Res Mechanica 6 (1983) 167. AECL Report, AECL-7729, 1983 January.

3. I.J. Hastings, C.E.L. Hunt, J.J. Lipsett and R.D. MacDonald, "Tests to Determine the Release of Short-Lived Fission Products from UO_2 Fuel Operating at Linear Powers of 45 and 60 kW/m: Methods and Results," AECL Report, AECL-7920, 1985 September.

4. I.J. Hastings, C.E.L. Hunt, J.J. Lipsett and R.G. Gray, "Transient Fission Product Release During Dryout in Operating UO_2 Fuel," International Meeting on Thermal Nuclear Reactor Safety, Chicago, Illinois, 1982 August 29-September 2, AECL Report, AECL-7832, 1982 December.

5. J.J. Lipsett, C.E.L. Hunt and I.J. Hastings, "Transient Fission Product Release Within Operating Fuel Elements During Power Cycles," OECD-NEA-CSNI/IAEA Specialists Meeting on Water Reactor Fuel Safety and Fission Product Release in Off-Normal and Accident Conditions, Riso, Denmark, 1983 May 16-20. AECL Report, AECL-8069, 1983 May.

6. I.J. Hastings, C.E.L. Hunt and J.J. Lipsett, "Release of Short-Lived Fission Products from UO_2 Fuel: Effects of Operating Conditions," Journal of Nuclear Materials, 130 (1985), 407.

7. P.J. Fehrenbach, I.J. Hastings, J.A. Walsworth, R.C. Spencer, J.J. Lipsett, C.E.L. Hunt and R.D. Delaney, "Zircaloy-Sheathed UO_2 Fuel Performance During In-Reactor LOCA Transients," Fifth International Meeting on Thermal Nuclear Reactor Safety, 1984 September 9-13, Karlsruhe, FRG. AECL Report, AECL-8569, 1984 October.

8. I.J. Hastings, C.E.L. Hunt, J.J. Lipsett, R.D. Delaney, P.J. Fehrenbach and L.L. Larson, "Behaviour of Short-Lived Fission Products Under Fuel Accident Conditions: Chalk River Studies," Canadian Nuclear Society Sixth Annual Conference, 1985 June. AECL Report, AECL-8773, 1985 January.

9. M.J.F. Notley, R. Deshaies and J.R. MacEwan, "Measurements of the Fission Product Gas Pressure Developed in UO_2 Fuel Elements During Operation," AECL Report, AECL-2662, 1967.

10. C.E.L. Hunt, J.C. Wood, B.A. Surette and J. Freire-Canosa, "Seventeen Years of Experience With Storage of Irradiated CANDU Fuel Under Water," Corrosion 81, National Association of Corrosion Engineers, April 6-10, 1981. AECL Report, AECL-7928, 1981 January.

11. C.E.L. Hunt, J.J. Lipsett and I.J. Hastings, "Release of Short-Lived Fission Products From Operating UO_2 Fuel Under Oxidizing Conditions," ANS Topical Meeting on Fission Product Behaviour and Source Term Research, 1984 June 15-19, Snowbird, Utah.

12. Hj. Matzke, "Atomic Transport Properties in UO_2 and Mixed Oxides (U, Pu) O_2," J. Chem Soc., Faraday Trans. 2, 1987, 83, 1121.

13. M.A. Mansouri, "Release of Fission Products From Lightly-Irradiated UO_{2+x}," PhD Thesis, University of California, Berkeley, 1995.

8. ACKNOWLEDGEMENTS

The authors would like to thank Atomic Energy of Canada Limited for making data available for this analysis, and in particular D.S. Cox for helpful discussions. This analysis was funded by the Academic Research Program of the Department of National Defence of Canada (allocation No. 3705-882) and the National Sciences and Engineering Research Council of Canada (award No. OG0155726).

TABLE 1
EXPERIMENTAL DETAILS

Characteristic	CRL Experiment designation			
	FIO-122	FIO-124	FIO-133	FIO-134
Fuel	UO2	UO2	UO2	UO2
Enrichment	5.02	4.5	1.38	5.98
Density (Mg/m3)	10.71	10.65	10.65	10.64
Grain size (μm)	7	7	7.6	10
Pellet diameter (mm)	12.16	12.16	18.09	11.63
Fuel stack length (mm)	477	477	378	477
Number of swept grooves	6	4	3	3
Groove dimensions (mm)	1.15 x 1.15	1.15 x 1.15	1.3 x 1.0	1.3 x 1.0
Sheath	Zircaloy-4	Zircaloy-4	304L SS	304L SS
Outside diameter (mm)	13.11	13.11	19.85	13.06
Wall thickness (mm)	0.43	0.43	0.82	0.635
Coolant	Pressurized water	Pressurized water	Pressurized water, fog.	Pressurized water
Pressure (MPa)	8.5	8.5	8.5	8.5
Flow (kg/s)	1.1	1.1	0.24	0.24
Inlet temperature (°C)	240	240	260-275	260
Linear power range (kW/m)	39 - 45	58 - 63	52 - 62	52 - 61
Final burnup (MWh/kgU)	86	50	54.9	227
Total shutdowns	27	18	31	34
Shutdowns with data	3	4	16	12
Startups with data	6	6	15	10

TABLE 2
SUMMARY OF STABLE GAS RELEASE

Experiment	Percent Xenon released			3/4 of the time to complete sintering (h)
	Measured %	Calculated %		
		All Shutdowns and Startups	Allowing 3/4 of the time to complete sintering	
FIO-122	1.3 - 2	1.53	0.78	46
FIO-124	2.2 - 2.5	1.69	1.02	15
Bundle SCA				
Outer elements	15.15 - 20.15	46.2	24.6	22
Inner elements	0.04 - 0.62	6.8	2.37	65

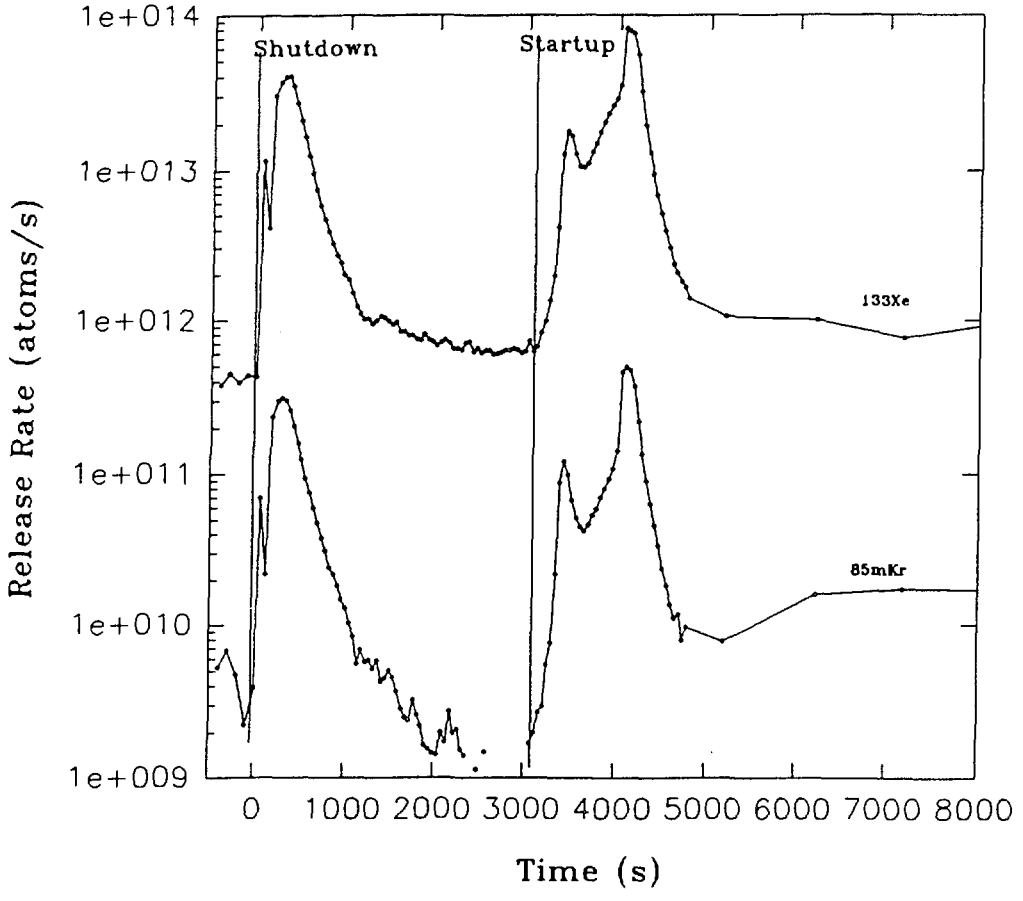

Figure 1: Shutdown and startup release rate versus time for 1981 November 16. The previous steady-state fuel power was 62 kW/m, and the burnup was 42 MWh/kgU. 19 h of operation had elapsed since the last startup.

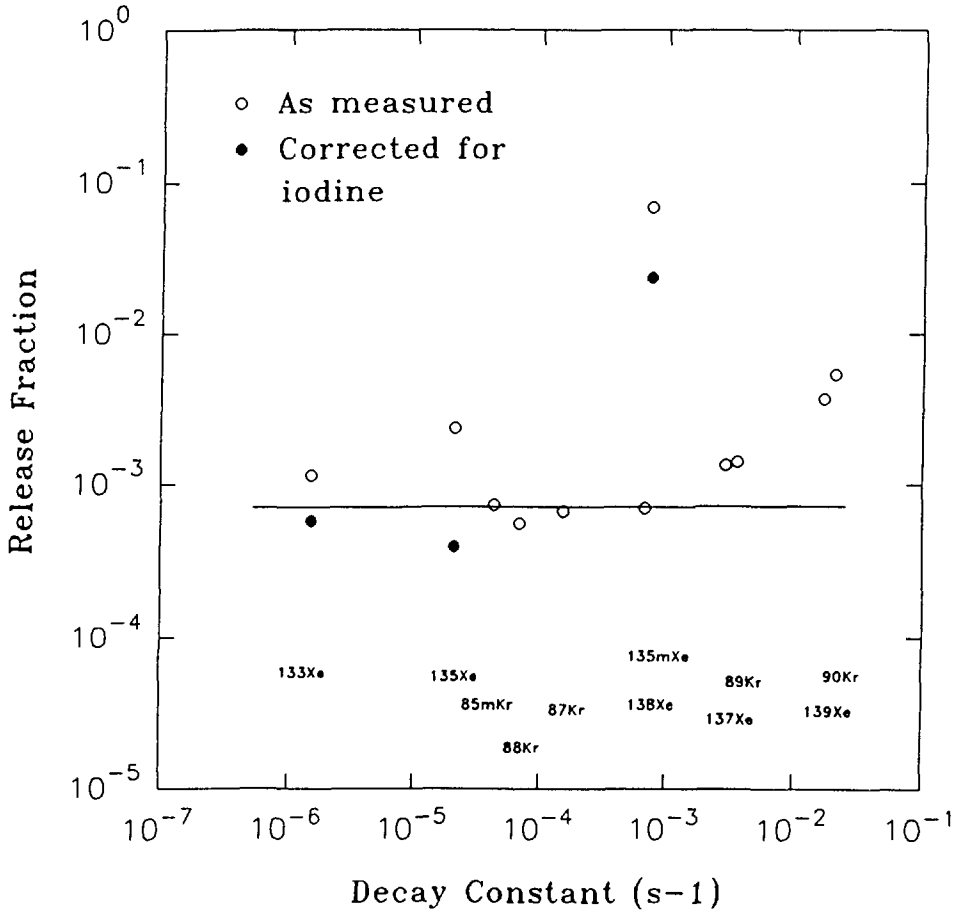

Figure 2: Shutdown release fractions for FIO-134 on 1982 October 24. 121.4 h had elapsed since the last startup. The previous steady-state power was 55 kW/m, and the burnup was 99 MWh/kgU.

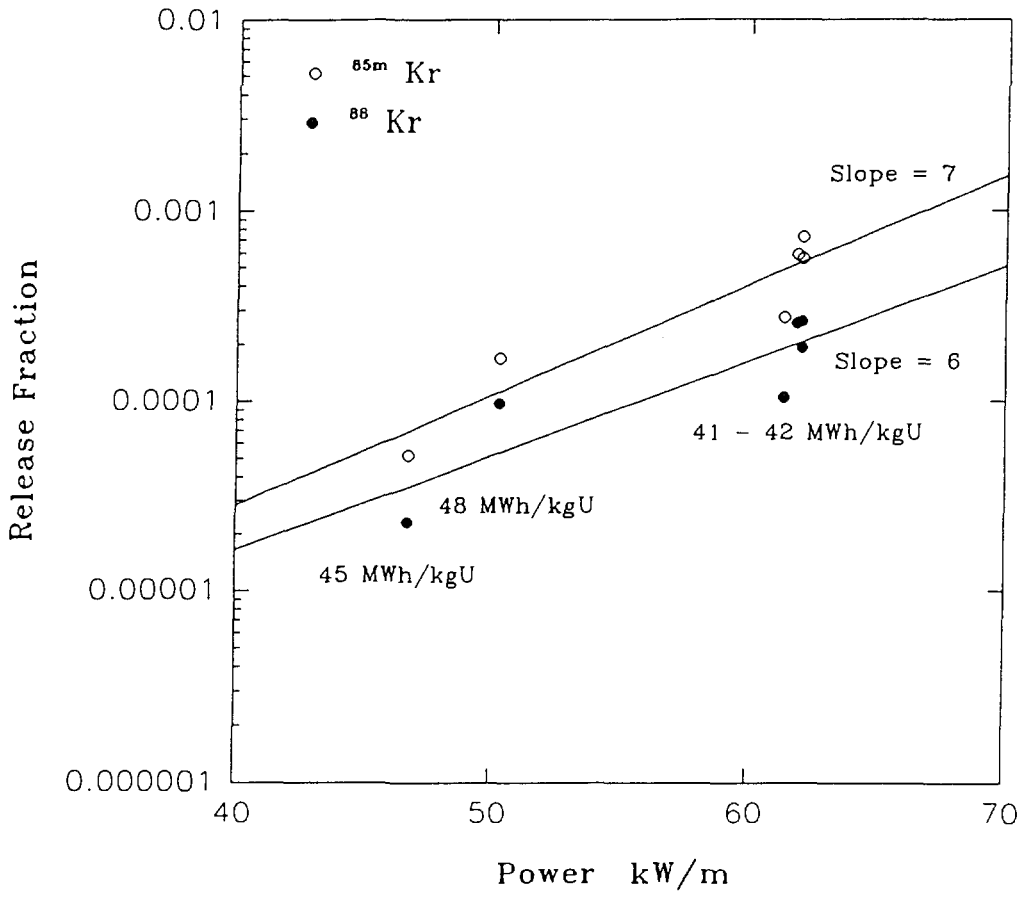

Figure 3: Release fraction versus fuel power at approximately constant burnup for two krypton isotopes. Data from FIO-133.

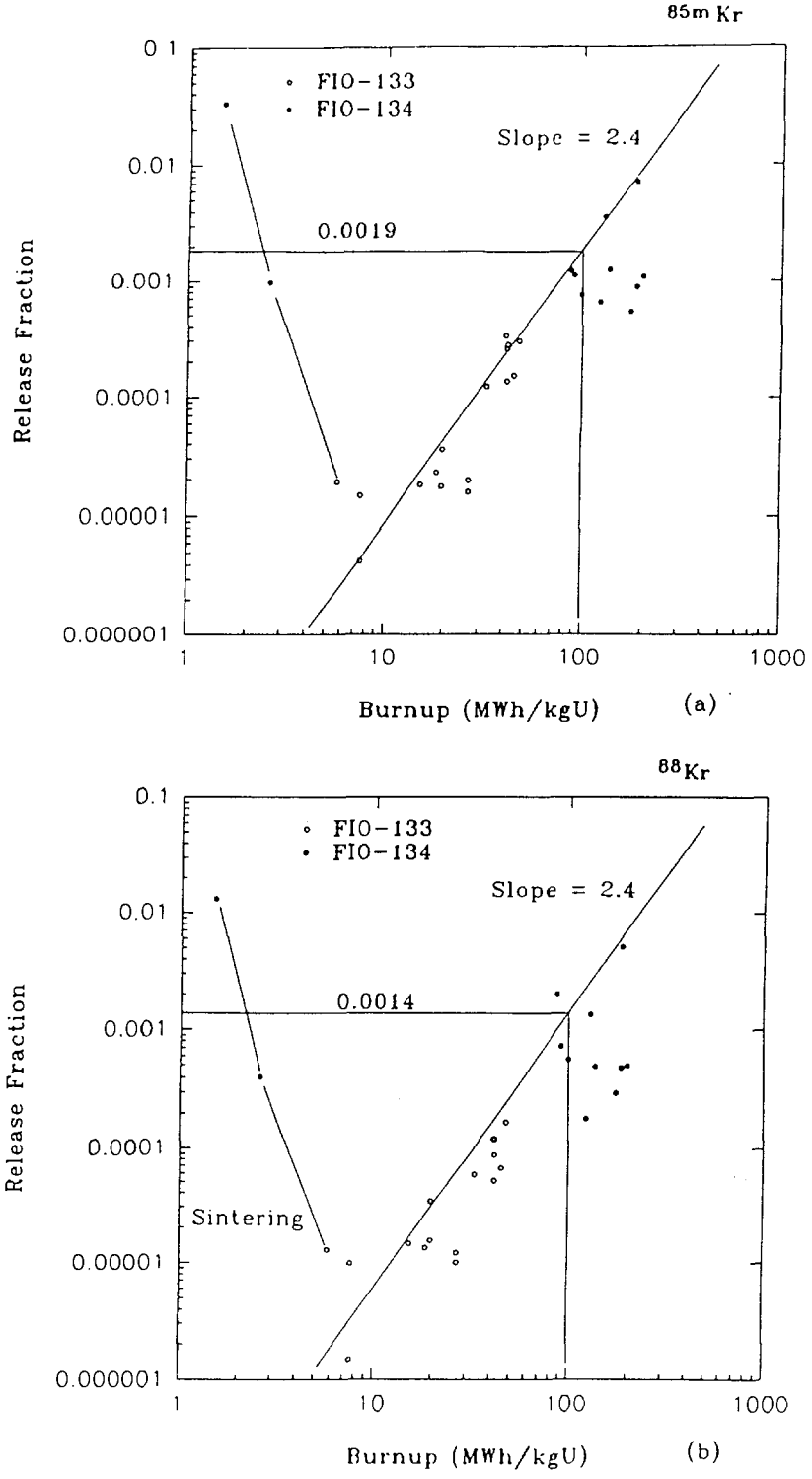

Figure 4: Burnup dependence of release fraction corrected to 55 kW/m fuel power for the isotopes
(a) ^{85m}Kr
(b) ^{88}Kr

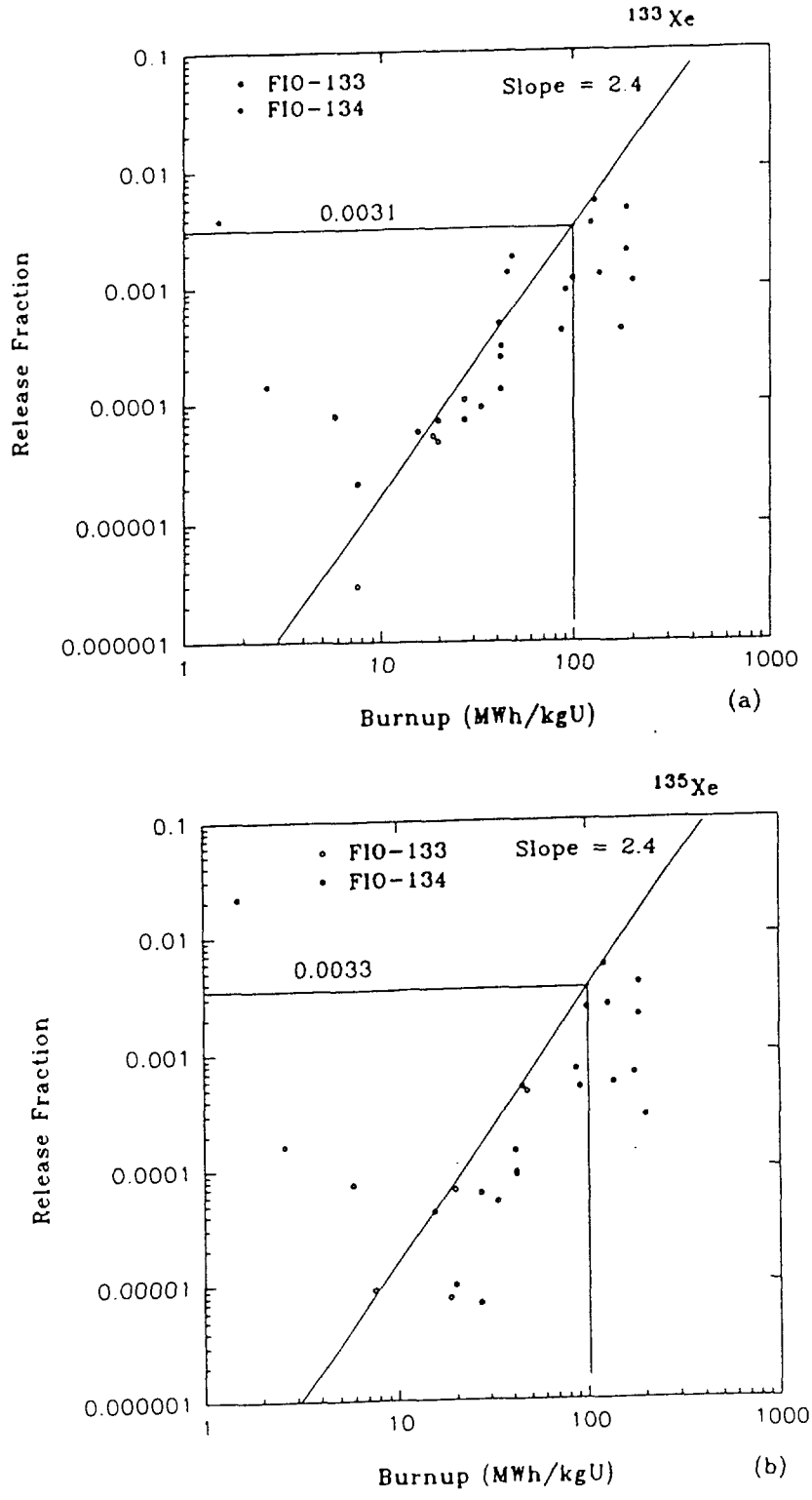

Figure 5: Burnup dependence of release fraction corrected to 55 kW/m fuel power for the isotopes
(a) ^{133}Xe
(b) ^{135}Xe

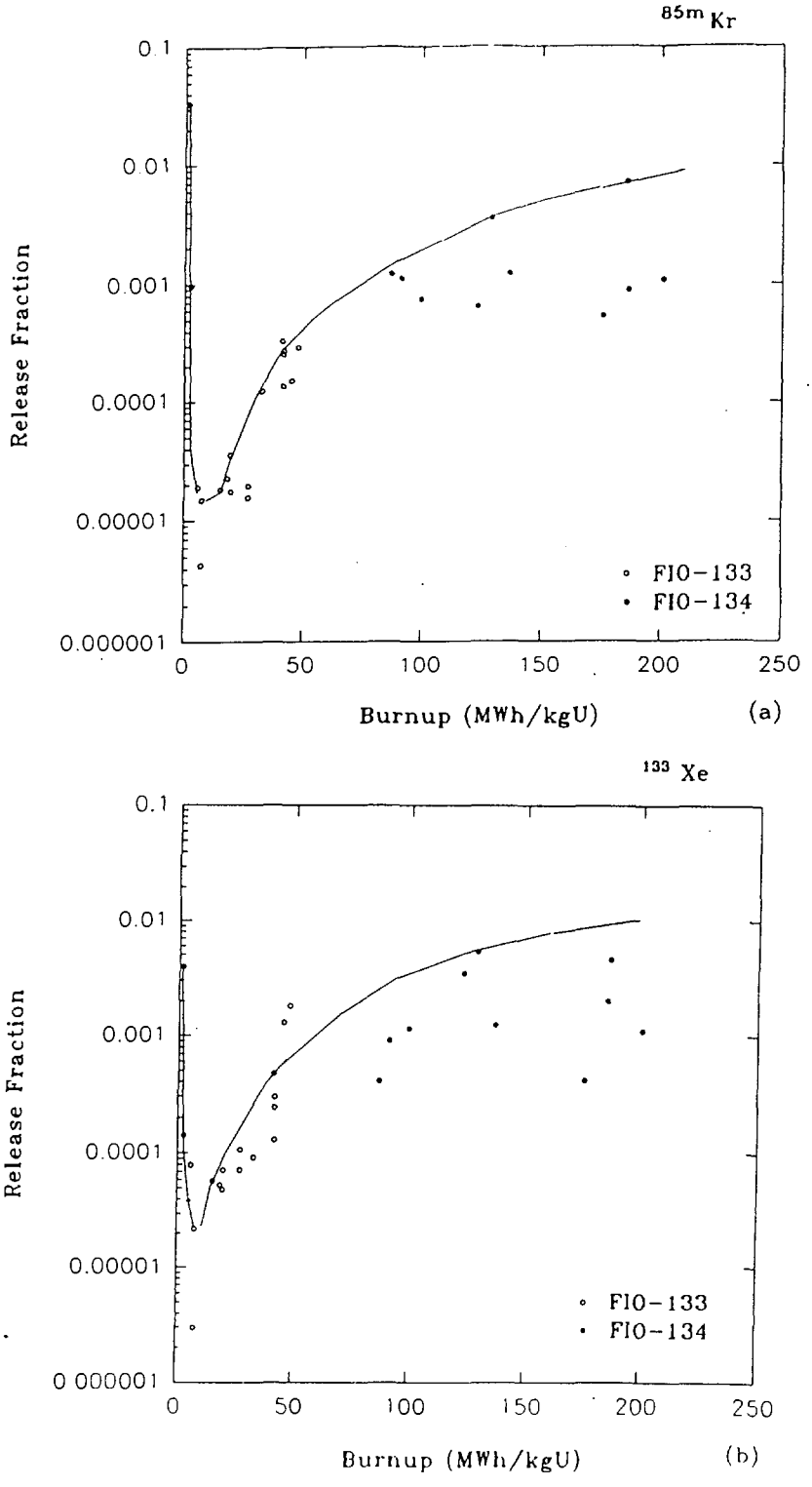

Figure 6: Burnup dependence of release fraction corrected to a fuel power of 55 kW/m for the isotopes
(a) ^{85m}Kr
(b) ^{133}Xe

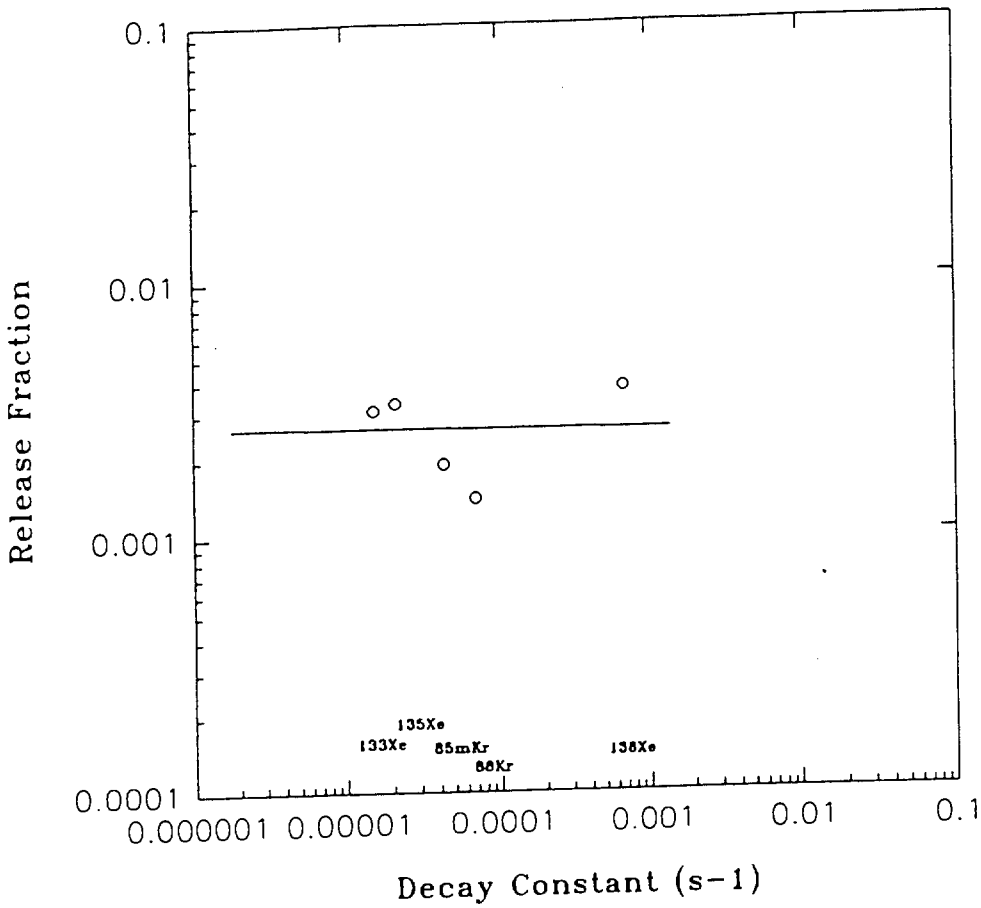

Figure 7: Shutdown release fractions calculated at 55 kW/m fuel power and 100 MWh/kgU burnup.

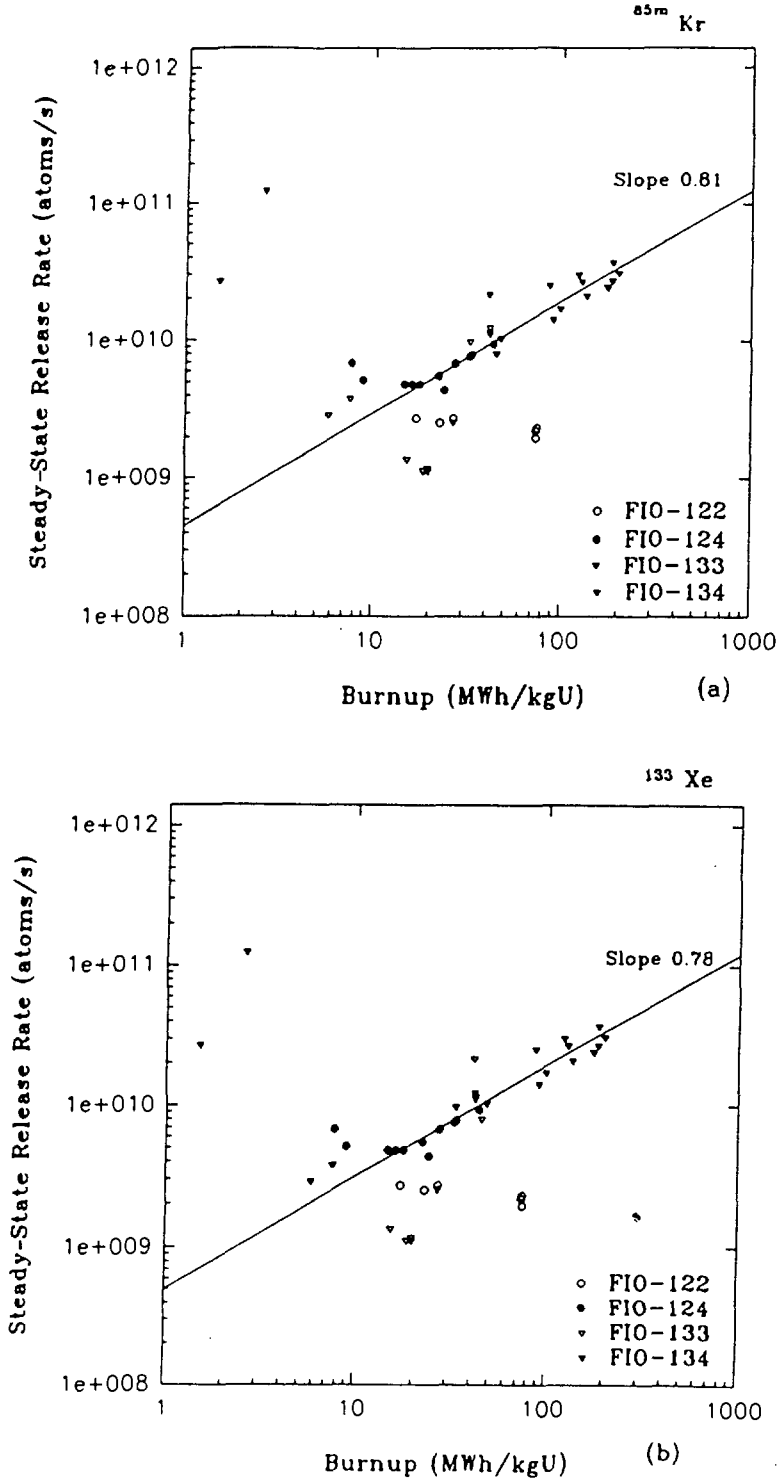

Figure 8: Steady-state release rate normalized to 477 mm fuel length and six swept grooves (1.15 mm x 1.15 mm) for the isotopes
(a) ^{85m}Kr
(b) ^{133}Xe

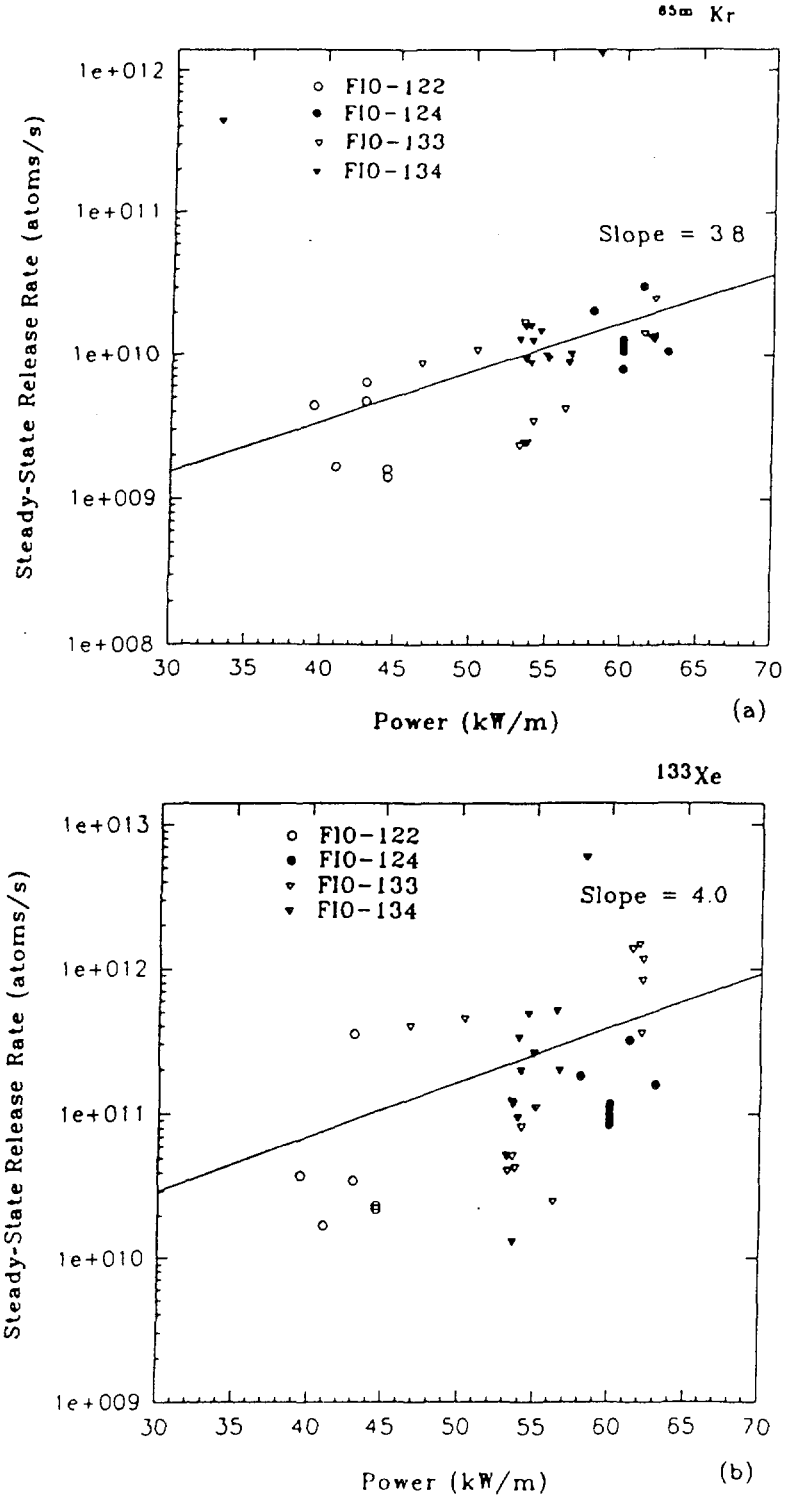

Figure 9: Steady-state release rate normalized to 50 MWh/kgU burnup for the isotopes
(a) ^{85m}Kr
(b) ^{133}Xe

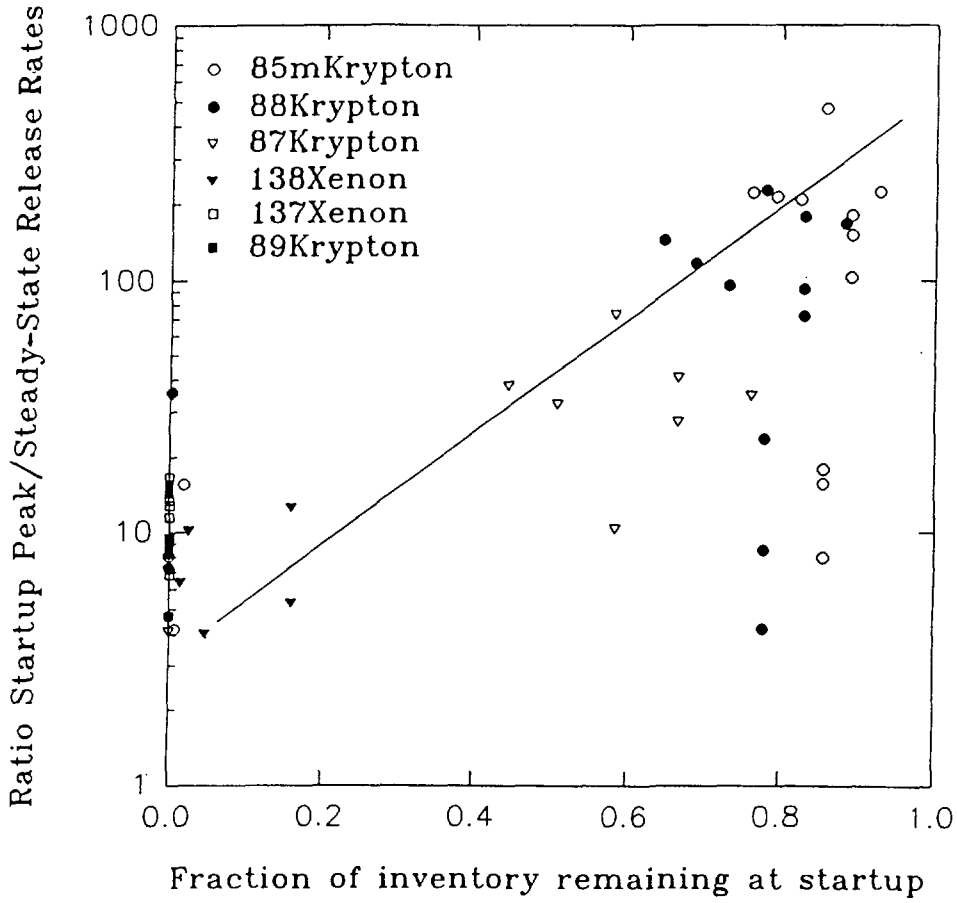

Figure 10: Ratio of startup peak release rates to the steady-state release rate at the same power as the peak, for short-lived isotopes with short-lived precursors. Data from FIO-133 and FIO-134.

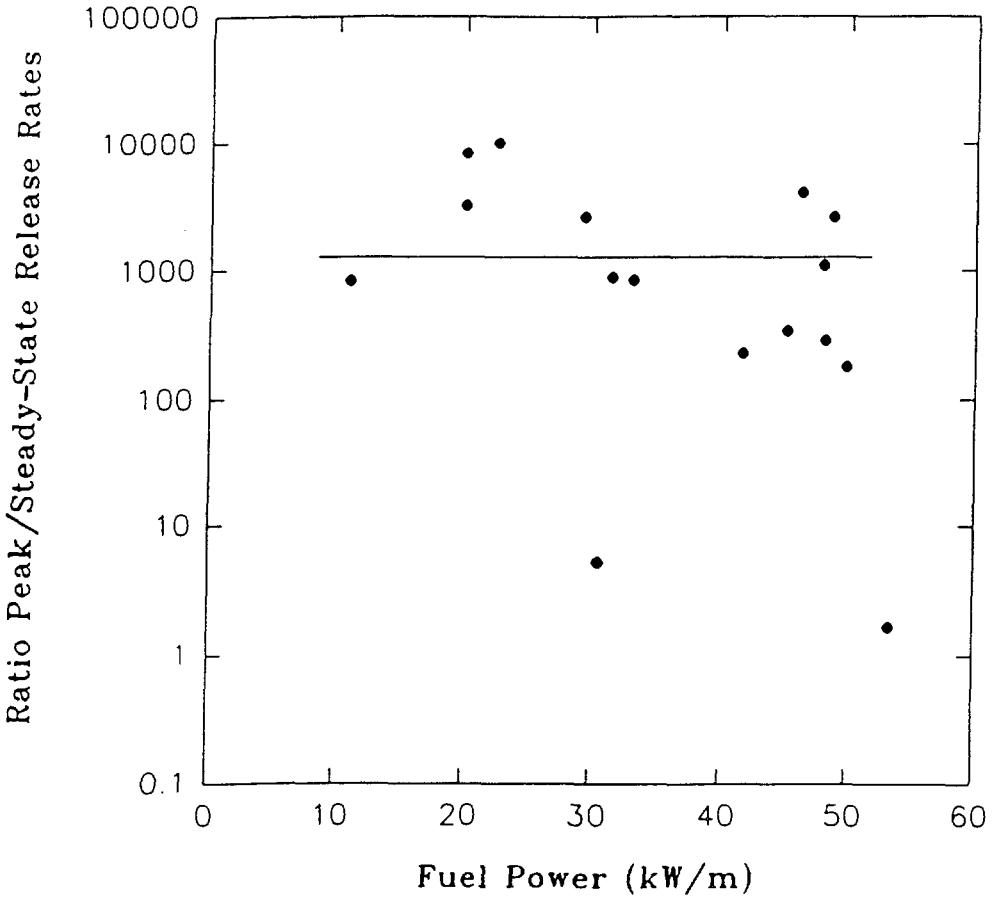

Figure 11: Ratios of the peak to the steady-state release rates at the power when the peak release was observed. Data for ^{133}Xe from FIO-133 and FIO-134.

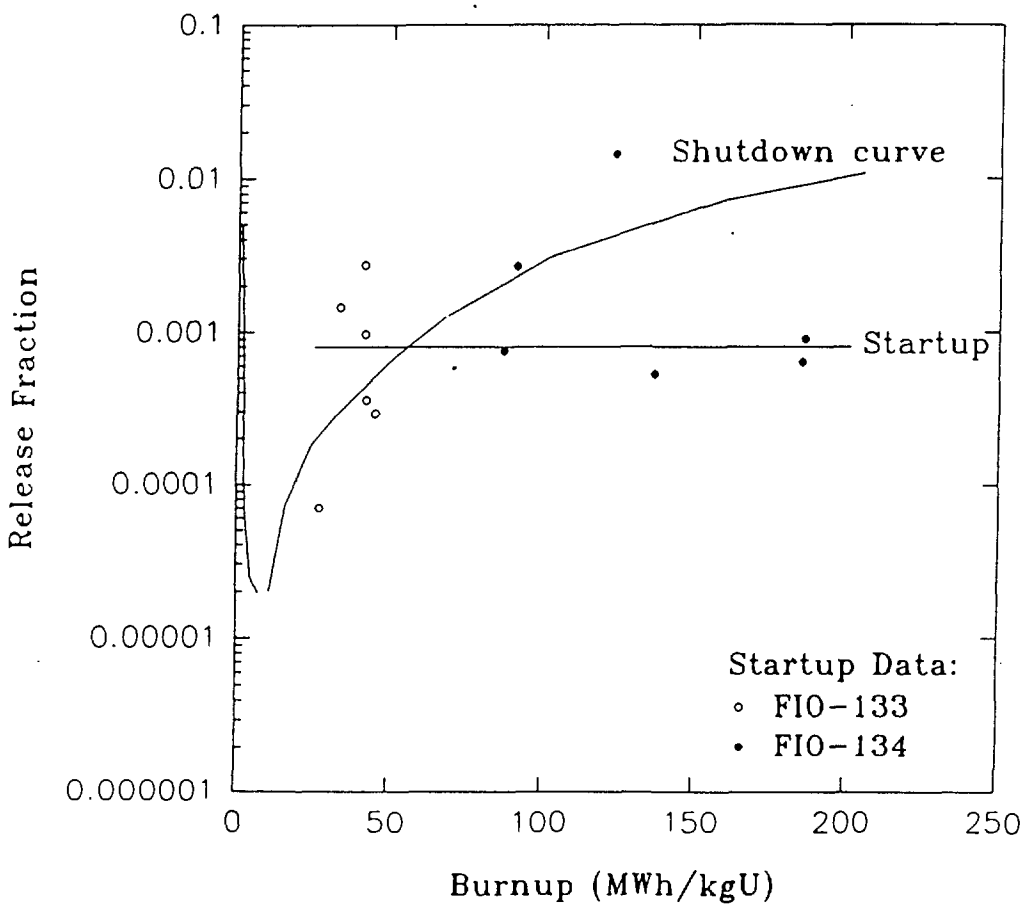

Figure 12: Startup release fraction versus burnup for ^{133}Xe. The shutdown curve from Figure 6(b) is included for comparison.

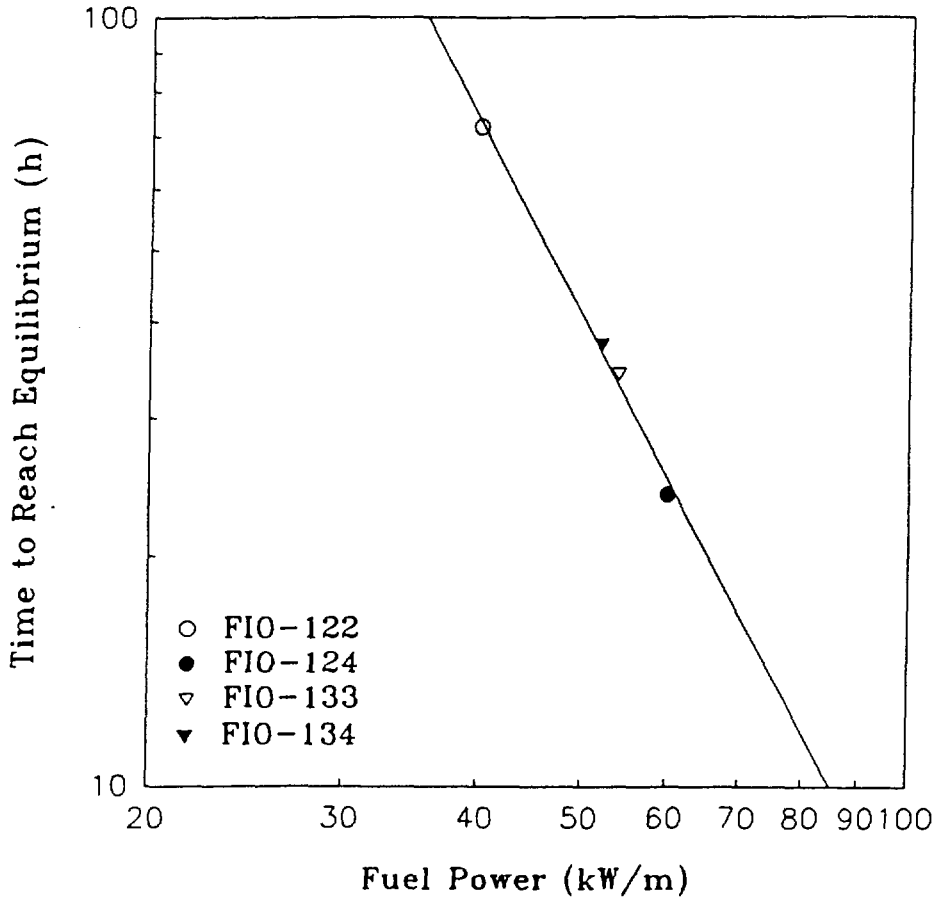

Figure 13: Estimated time required to resinter fuel cracks after reactor startup as a function of the fuel operating power, based on ^{135}Xe data.

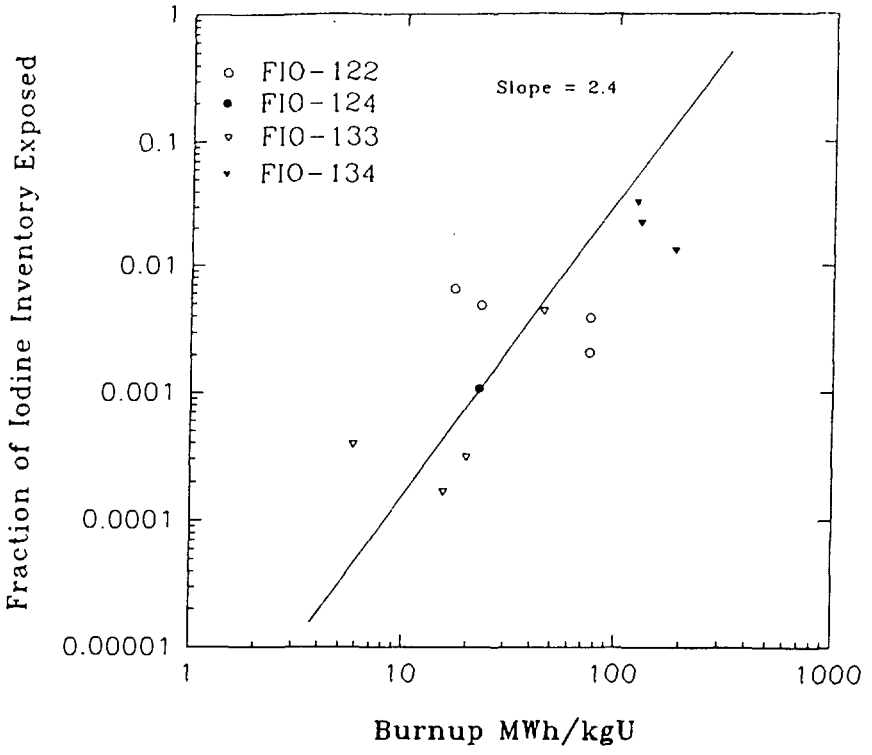

Figure 14(a): Total fraction of iodine inventory exposed on shutdown corrected to 55 kW/m by $(\text{Power})^{6.5}$.

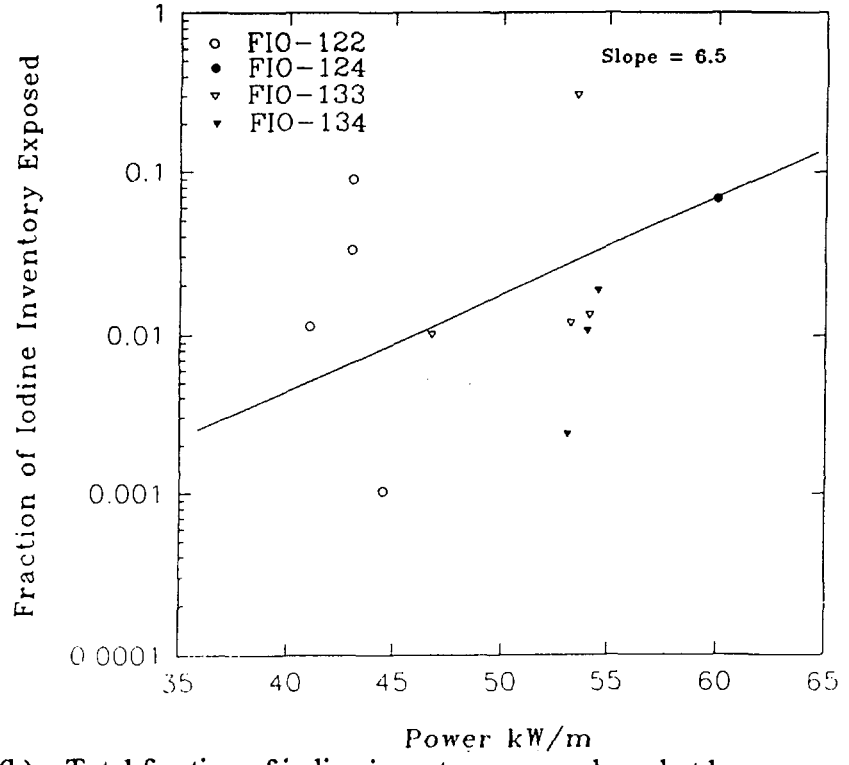

Figure 14(b): Total fraction of iodine inventory exposed on shutdown corrected to 100 MWh/kgU by $(\text{Burnup})^{2.4}$.

ISSN 0067-0367

To identify individual documents in the series, we have assigned an AECL- number to each.

Please refer to the AECL- number when requesting additional copies of this document from:

Scientific Document Distribution Office (SDDO)
AECL
Chalk River, Ontario
Canada K0J 1J0

Fax: (613) 584-1745 Tel.: (613) 584-3311
ext. 4623

Price: A

Pour identifier les rapports individuels faisant partie de cette serie, nous avons affecté un numéro AECL- à chacun d'eux.

Veuillez indiquer le numéro AECL- lorsque vous demandez d'autres exemplaires de ce rapport au:

Service de Distribution des Documents Officiels
EACL
Chalk River (Ontario)
Canada K0J 1J0

Fax: (613) 584-1745 Tél.: (613) 584-3311
poste 4623

Prix: A